Electron transfer induced side-chain cleavage in tryptophan facilitated through potassium induced transition-state stabilization in the gas-phase

F. Ferreira da Silva[*,#], T. Cunha[#], A. Rebelo[#], A. Gil[†,⊥], M. J. Calhorda[†], G. García[‡], O. Ingólfsson[±] and P. Limão-Vieira*[*,#]*

[#] Atomic and Molecular Collisions Laboratory, CEFITEC, Department of Physics, Universidade NOVA de Lisboa, 2829-516 Caparica, Portugal.

[†] BioISI -Biosystems & Integrative Sciences Institute, Departamento de Química e Bioquímica, Faculdade de Ciências, Universidade de Lisboa, Campo Grande, 1749-016 Lisboa, Portugal

[⊥] CIC nanoGUNE BRTA, Tolosa Hiribidea, 76, E-20018, Donostia – San Sebastián, Euskadi, Spain

[‡] Instituto de Física Fundamental, Consejo Superior de Investigaciones Científicas (CSIC), Serrano 113-bis, 28006, Madrid, Spain

[±] Chemistry and Science Institute, University of Iceland, Dunhagi 3, 107, Reykjavik, Iceland

ABSTRACT

Fragmentation of transient negative ions of tryptophan molecules formed through electron transfer in collisions with potassium atoms is presented for the first time in the laboratory collision energy range from 20 up to 100 eV. In the unimolecular decomposition process, the dominating side chain fragmentation channel is assigned to the dehydrogenated indoline anion, in contrast to dissociative electron attachment of free low-energy electrons to tryptophan. The role of the collision complex formed by the potassium cation and tryptophan negative ion in the electron transfer process is significant for the mechanisms that operate at lower collision energies. At those collision times, on the order of a few tens of fs, the collision complex may not only influence the lifetime of the anion, but also stabilize specific transition states and thus alter the fragmentation patterns considerably. DFT calculations, at the BHandHLYP/6-311++G(3df,2pd) level of theory, are used to explore potential reaction pathways and the evolvement of the charge distribution along those.

Introduction

Charge transfer reactions are ubiquitous in nature and play an essential role in living organisms by maintaining the functionality and, not less important, the selectivity of biologically active molecules (see Refs.[1–4] and references therein). These processes can be of high complexity and may proceed via numerous steps, e.g. in cellular respiration more than 15 electron transfer steps occur (see Ref.[5] and references therein). Often there are specific molecular entities or redox systems that play essential roles in those electron transfer processes, among them the aromatic amino acid redox-pair tryptophan and tyrosine (Ref.[4,6–8] and references therein). From these, the former contains an indole moiety linked to the α-C through a methylene bridge at the C_3 position. The latter contains a phenol moiety linked to C_α through a methylene bridge in *para*-position.

Notwithstanding, the indole moiety plays an essential role in a vast variety of physiologically active substances.[9] The simpler natural ones include such important compounds as serotonin and melatonin and applications of drugs containing the indole moiety are found in cancer therapy, depression, migraine and rheumatism treatments. However, the most "far out" example of physiologically active substances containing the indole moiety is the lysergic acid diethylamide (LSD).

Within this context, and the potential role of low-energy electrons in radiation damage to biological systems,[10] a significant number of gas-phase studies have been performed to investigate low energy electron interactions with isolated biologically relevant molecules (see e.g. reviews in Refs. [11–14] and references therein). While such gas-phase studies do generally not allow for replication of the actual biological environment of these molecules, they have the advantage to be performed under well-controlled experimental conditions.[15] Hence, gas-phase studies may offer insight into fundamental processes, which are not attainable when those molecules are embedded in their natural environment. For low-energy electron interactions with tryptophan, we note studies on electron transmission mapping the low-lying temporary anion states by Aflatooni *et al.*[16] and an electron energy loss study by Borisevich *et al.*. [17] Furthermore, a number of electron attachment studies have been reported on tryptophan [18–20], its methyl ester[19] and N-acetyl tryptophan. [21] Also electron stimulated desorption (ESD), from condensed films of tryptophan, has been reported for the electron energy range from 0 to 12 eV.[22] As far as indole is concerned, a number of studies have been reported on its interaction with low energy electrons. These include a combined electron transmission and dissociative electron attachment (DEA) study by Modelli *et al.*[23] (also including indoline), an electron energy loss spectroscopy (EELS) study by Borisevich *et al.*[17], calculation of the total electron scattering cross sections by Chiari *et al.*[24] (used to determine the dipole-bound

electron affinity of indole), a Rydberg electron transfer study by Carles *et al.* [25] and an ultrafast electron diffraction study by Park *et al.*[26]

In electron transmission spectroscopy (ETS), Aflatooni *et al.*[16] observe the lowest lying negative ion resonance of tryptophan to be at about 0.7 eV and they find the next higher lying negative ion state at ~1.6 eV. The former is assigned to a π_1^* antibonding orbital localized on the indole moiety, while the latter is interpreted to be composed of π_2^* and π_3^* anti-bonding orbitals localized on the indole and carbonyl moieties, respectively. This is in good agreement with the electron transmission spectra of indole and formic acid, where these resonances appear at 1.85 and 1.73 eV, respectively.[16,23] Additional information supporting this assignment is found by comparing the contribution in the ETS of tryptophan to the same contributions in indole and the aliphatic amino acids, where they are shifted to higher energies as compared to tryptophan. Note in this context, that the indole-based resonances are shifted to lower energies by about 0.2 eV in tryptophan, while the π^* carboxyl resonance is shifted to higher energies in the aliphatic amino acids (also about 0.2 eV). Further resonances are observed in the ETS of tryptophan, at 2.5 eV (2.7 eV in indole) and close to 3.5 eV. The former is assigned as a π_4^* shape resonance and the latter is tentatively assigned as a core excited resonance associated with one of the low-lying electronic states. The 3.5 eV resonance agrees well with the EELS of tryptophan[17] where the first transition is observed close to 3.2 eV and that of indole where this transition is observed at about 3.3 eV and is associated with a transition to the first triplet state. In dissociative electron attachment the total cross-section for the dominant anion formation from tryptophan is found to peak at 1.2 eV, while Vasil'ev *et al.*[19] find the loss of a hydrogen atom from tryptophan and its methyl ester at 1.2 and 1.55 eV, respectively. This is consistent with the interpretation of tryptophan ETS where the resonance observed at 1.6 eV was assigned to an overlapping contribution from π orbitals at the indole ring

and the carboxyl group. Hence, it apparently proceeds from the indole moiety as well as from the carboxyl group. Note that while ETS reflects the whole width of the respective resonances, DEA competes with autodetachment, i.e. ejection of the extra electron, which is most efficient at higher energies. Thus, the DEA ion yield generally appears at lower energies than the actual position of the respective resonances. In addition to hydrogen loss, Vasil'ev *et al*.[19] also observe the cleavage of the carboxyl group from the α-carbon, formation of fragments from the carboxyl group and cleavage of the bond from the methylene bridge (β-carbon) to the α-carbon of the backbone. In an earlier study, Abdoul-Carime *et al*.[18] have reported that hydrogen loss is only a minor channel and formation of $HCOO^-$ is found to be the most pronounced channel. Bond cleavage from the methylene side group bridge to the α-carbon of the backbone is also observed in this study as well as the typical carboxyl fragments. In addition, Abdoul-Carime *et al*.[18] observe CN^- formation peaking at 1.2 eV, a fragment anion that requires considerable rearrangement of the TNI formed in the free electron attachment process. This has been discussed in detail for the aliphatic amino acids glycine and valine.[27–29] In ESD from condensed layers of tryptophan,[22] the most pronounced channel is assigned to H^-, yet other fragment anions are also discernible, O^-, OH^- and CN^-. These fragment anions are observed at considerably higher energies than in the gas-phase, which is predominantly attributed to the energetic constraints on the desorption process. Finally, it is worth noting that the photolysis of jet-cooled tryptophan at 212.8 and 193 nm,[30] yields C_α and C_β bond cleavage as the only fragmentation pathway. A certain analogy may be expected between such photolysis experiments and dissociation through free electron attachment as the former often corresponds to the promotion of an electron from a bonding orbital to an anti-bonding orbital, while the later may constitute an extra electron occupying the same anti-bonding orbital. However, in the photolysis study referred here above, the dissociation is attributed to the ground state of the

molecule after rapid internal conversion rather than direct dissociation along an anti-bonding excited state.

In this contribution, we study negative ion formation and decay channels of tryptophan in electron transfer processes. We argue that the ion-pair/polarization-interaction in the collision complex may not only influence the lifetime of the anion formed in the electron transfer process, but may also stabilize specific transition states and thus alter considerably the fragmentation patterns. These findings are discussed in context of DFT calculations carried out for potential reaction pathways and the relative stabilization of the corresponding transition states. Electron transfer experiments are in many ways complementary to studies of anion formation and decay through free electron attachment, as the lifetime of the negative ion initially formed in collisions with potassium may be extended considerably by stabilization through polarization interaction in the transient collision complex (see Refs.[31–33]), as compared to that of the transient negative ion (TNI) formed in free electron attachment. Moreover, as the interaction time of the potassium can be tuned through the collision energy, such experiments allow differentiating between slower, often kinetically hindered channels and faster, more direct channels. Recently, such influence of the extended lifetime of the TNI formed in collision with potassium has been demonstrated for the aliphatic amino acids glycine[34] and alanine (not observed in valine),[35] tyrosine[36] and the nucleobases thymine and uracil.[32–34] Specifically, for thymine, an unambiguous comparison has been offered of negative ion formation through collisions with potassium, dissociative electron attachment and metastable decay of the thermally activated thymine anion in its electronic ground state.[37] Distinct site selectivity in bond breaking was also shown in electron transfer experiments by selective N-methylation of pyrimidines[37,38] and in DEA to simple organic molecules, such as acetic acid.[39] Furthermore, in a comprehensive electron transfer study on uracil (U) and its

halogenated derivatives, 5-chlorouracil (5-ClU) and 5-fluorouracil (5-FU),[40] a significant enhancement of the electron transfer process was inferred for the Cl⁻ channel from 5-ClU when the transient time of the potassium was on the same order as the C−Cl vibrational period.

Hence, the transition time of the potassium is not only expected to influence the lifetime of the TNI, as compared to free electron attachment, but may also influence the underlying collision dynamics of the electron transfer process, i.e. diabatic and/or adiabatic descriptions may hold.

Methods

Experimental

The experimental setup has been described in detail elsewhere,[31] and we thus only give a brief description here. In this setup, K^+ ions produced in a commercial potassium ion source (STD 250 K Ion source from HeatWave Labs, Inc. US) are accelerated to 20–100 eV before passing through an oven containing neutral potassium vapour. In the oven, the potassium ions resonantly charge-exchange with the neutral potassium, producing a beam of hyperthermal, neutral potassium atoms. Residual ions, from the primary beam, are removed by electrostatic deflection plates placed outside the oven. The intensity of the neutral potassium beam is monitored using a Langmuir-Taylor ionisation detector, before and after the TOF mass spectra collection, with typical values of tens of pA. The effusive beam of tryptophan was generated through sublimation of the solid sample at 490 K and the heating temperature was controlled using a proportional integral derivative controller unit. In order to test for any thermal decomposition, control spectra were recorded at different temperatures. No differences were observed in relative peak intensities as a function of the temperature. In order to prevent any sample deposition and thence charge accumulation on the

electrodes, the extraction region and the TOF system were heated to approximately 393 K throughout the measurements.

The effusive beam of tryptophan enters the collision zone through a 1 mm diameter capillary, where it crosses the neutral hyperthermal potassium beam between two parallel plates with 1.2 cm separation. The anions produced were extracted by a 250 Vcm^{-1}, pulsed electrostatic field. The typical base pressure in the collision chamber was 8×10^{-6} Pa and the working pressure did not rise significantly upon heating the powder tryptophan sample. Mass spectra were obtained by subtracting the background measurements (without heated sample) from measurements with the sample present. The mass calibration was carried out on the basis of the well-known anionic species formed after potassium collisions with nitromethane.[31] Tryptophan was purchased from Sigma-Aldrich with a ≥ 99.5 % stated purity and used as delivered.

Computational Studies

In order to evaluate the reaction paths initiated by hydrogen transfer from the side chain to the indole moiety a set of DFT calculations were performed with the Gaussian09 software.[41]

The single bonds corresponding to the backbone of tryptophan and the two single bonds not included in the aromatic system of its side-chain are free to rotate. The energy of these torsions is on the order of tens to hundreds of meV, thus giving rise to different stable rotamers. Keeping this in mind, a systematic conformational search was performed, using the Avogadro software.[42] The C-OH bonds were considered as being two fold (rotations of 180°), while the remaining single bonds were considered as being three fold (rotations of 120°). This amounts to 108 starting conformers, which were subjected to minimization by molecular mechanics using the force field MMFF94.[43,44] At the end, as some of these rotamers evolved to the same structure, a total of 46 structures showed nuclear stability. These 46 structures were optimized at the DFT level of theory

with the BHandHLYP functional and the 6-311++G(3df,2pd) basis set. The respective radical anions were then generated from all the optimized neutral systems by addition of one electron and re-optimized. The most stable anionic structure was chosen for the fragmentation study. The BHandHLYP functional was chosen because it is known that for open-shell systems, such as these radical anions, pure and hybrid density functionals with small percentage of exact exchange could lead to a bad description of the geometrical structure of the ground state of the system[45] and to molecular structures with a too much delocalized Singly Occupied Molecular Orbital (SOMO).[46–48]

The search for transition states of the reactions involving hydrogen transfer to the indole ring was carried out using Chemical Dynamics Simulations with TSSCDS software.[49,50] On the other hand, for the transition states involving C-C bond cleavage, the C-C distance (reaction coordinate) was increased in steps of 0.05 Å until the bond cleavage was complete. For each frozen C-C distance, the remaining degrees of freedom were allowed to relax, before the next step. The highest energy structure (top of the hill on the reaction coordinate) obtained, was then optimized as a transition state (saddle point). The transition states were optimized at BHandHLYP/6-311++G(3df,2pd) level of theory.

The nature of all stationary points was checked by vibrational frequency calculations. In all cases, intrinsic reaction coordinate (IRC) calculations were carried out to confirm that the located transition states linked the proposed reactants, intermediates and products. Thermodynamic corrections were computed assuming an ideal gas, unscaled harmonic vibrational frequencies and the rigid-rotor approximations by standard statistical methods[51]. It is known that atomic charges are not proper quantum observables and their assignment to atoms has been a problem, leading to several arbitrary approaches to obtain values for the charge distributions in such systems.

Sometimes the calculation of charges in different fragments of a system could even lead to contradictory conclusions[52,53]. For this reason, spin and charge density were evaluated by using different charge schemes based on several approaches of different nature. Thus, we used for the main qualitative discussion Mulliken[54] based on the population analysis of the wavefunction. Nevertheless, for comparison, charge density distributions were also evaluated by means of the following approaches: Hirshfeld approach[55] based on the electronic density of the molecule as a function of space and of a fictitious pro molecule that the method defines as the sum over the ground-sate atomic densities; APT approach[56] based on the atomic polar tensor, charge model-5 (CM-5)[57]; Merz-Singh-Kollman[58,59] where the charges are derived from an electrostatic potential; and NBA/NBO[60] where the charges are calculated from the so-called natural population analysis and are relatively insensitive to the basis set changes.

Results and discussion

Fig. 1 shows time-of-flight mass spectra (TOF-MS) of negative ions formation through electron transfer in potassium-tryptophan collisions at laboratory frame collision energies (E_{coll}) of 20, 50, 75 and 100 eV. In the centre-of-mass frame (E_{CM}) these correspond to 10.8, 33.4, 52.3 and 71.2 eV, respectively, representing the maximum energy transfer possible through collisional activation.
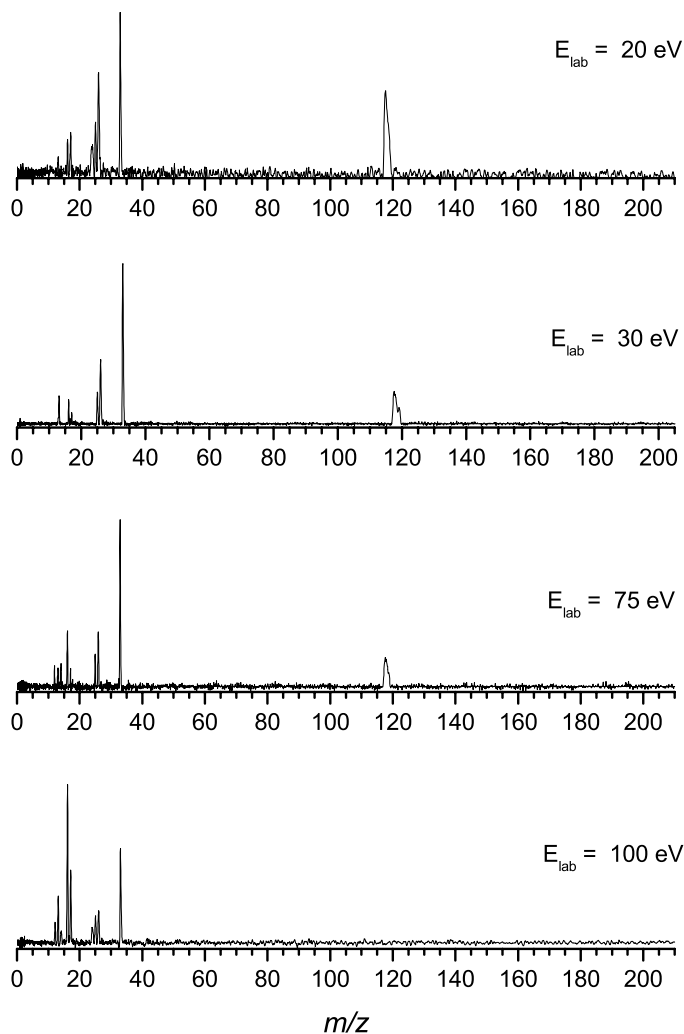

Figure 1. Negative ion mass spectra recorded at potassium–tryptophan lab-frame collision energies of 20, 30, 75 and 100 eV.

In the lower mass region, below m/z 100, the main fragments appear at m/z 16, 17, 26 and 33. These are assigned to O^-/NH_2^-, OH^-, $CN^-/C_2H_2^-$ and HO_2^-/NH_2OH^-, respectively. With the exception of HO_2^-/NH_2OH^-, all these fragments are observed in DEA to tryptophan,[18] (see Table 1) and in general from DEA to amino acids.[61,62] The isobaric fragments $CN^-/C_2H_2^-$ and O^-/NH_2^-, have been studied in detail, both in DEA to glycine [28] and to valine.[27] In both cases the total ion yield results from a combined contribution of these fragments but in the case of O^-/NH_2^-, NH_2^- dominates in the low-energy range, to about 6 eV incident electron energy, while O^- dominates above that energy. For $CN^-/C_2H_2^-$, CN^- dominates in the low-energy range and $C_2H_2^-$ in the high-energy range in the case of glycine. For valine, on the other hand, the situation is not as clear and both fragments are mainly formed below 4 eV incident electron energy. Further low intensity $C_nH_m^-$ fragments are also discernible in the mass spectra shown in Fig. 1. We attribute these to contributions from traces of pump oil in the chamber.

Table 1. Tryptophan anion formation upon electron transfer (ET, current results) compared to anion formation from Tryptophan through DEA (taken from ref. 18 and ref. 19). From ref. 19 the relative intensities reported are shown in parenthesis after the respective fragments and from ref. 18 the approximate count rates, reported as counts per second are shown in parenthesis after the respective fragments.

m/z	Anion		
	ET *present results*	DEA (ref. 18)	DEA (ref. 19)
203	-	[Try-H]⁻ (2)	[Try-H]⁻ (100)
182	-	-	[Try-H-H_2O]⁻ (< 1)
159	-	-	[$C_{10}H_{11}N_2$]⁻ (1.9)
158	-	-	[$C_{10}H_{10}N_2$]⁻ (1.5)
130	-	-	[C_9H_8N]⁻ (0.74)

m/z			
118	$[C_8H_7NH]^-$	-	-
74	-	$[C_9O_2H_4N]^-$ (15)	$[C_9O_2H_4N]^-$ (7.8)
45	-	$[CO_2H]^-$ (175)	$[CO_2H]^-$ (< 1)
33	$[HO_2]^-$/ $[OHNH_2]^-$	-	-
26	$[CN]^-$/ $[C_2H_2]^-$	$[CN]^-$/ $[C_2H_2]^-$ (4)	-
17	$[OH]^-$	$[OH]^-$ (4)	$[OH]^-$ (<1)
16	$[O]^-$/ $[NH_2]^-$	$[O]^-$/ $[NH_2]^-$ (4)	$[O_2]^-$/ $[NH_2]^-$ (< 1)

In the ET mass spectra (Fig. 1), there is no evidence of the dehydrogenated molecular anion (m/z 203) formation and for m/z > 100, the only fragment anion observed with appreciable intensity appears at m/z 118. We attribute this contribution to isomers of the dehydrogenated indoline anion, $C_8H_7NH^-$ (shown along with indole and tryptophan in Fig. 2). In one of these isomers the indoline anion has lost a hydrogen from C_3, in the other a hydrogen has been transferred to C_{3a}, leading to loss of the aromaticity and a hydrogen is removed from both C_2 and C_3. The formation of these anions is a remarkable process because: i) it requires rupture of the indole γ-C_3 bond to the C_β of the remaining amino acid moiety, while side chain cleavage in DEA and photolysis exclusively proceeds through rupture of the C_β–C_α bond[19] and ii) it requires the transfer of two hydrogen atoms to the indole moiety from the remaining amino acid. Furthermore, a close inspection of the mass spectra in Figure 1 shows that the relative intensity of this fragment anion decreases significantly with increasing collision energy. In fact, at 100 eV laboratory frame collision energy there are no signs of isomers of the dehydrogenated indoline anion at m/z 118.
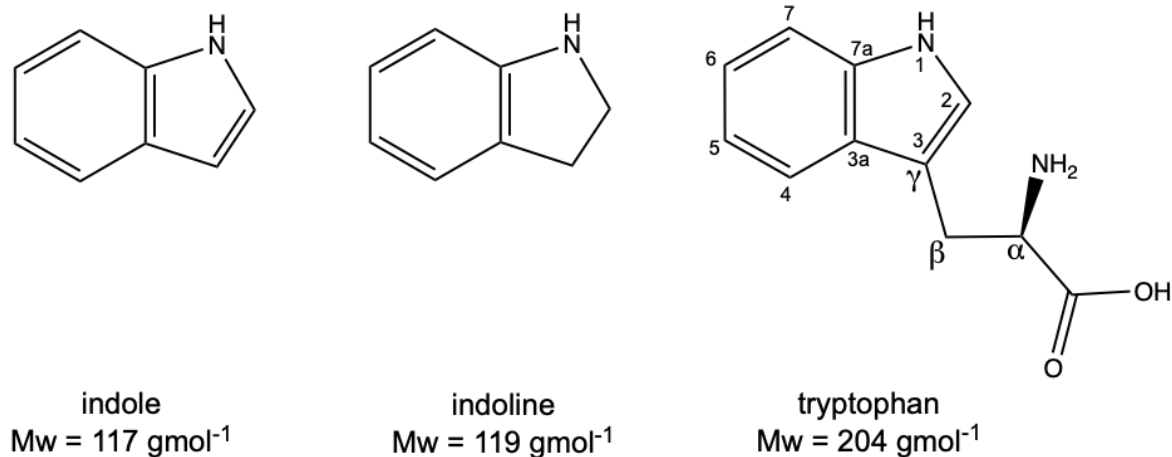
Figure 2. Molecular structures of indole, indoline and tryptophan. Assignments of the carbon atoms are shown on tryptophan structure.

For a more quantitative consideration, Fig. 3 shows the branching ratios (BRs) as a function of the collision energy for the dehydrogenated indoline anion (m/z 118) and for the fragments OH^- and O^-/NH_2^-. While formation of the dehydrogenated indoline anion requires the transfer of two hydrogen atoms from the backbone to the side chain (indole moiety), OH^- results from a direct dissociation process from the carboxyl group. This process also seems to be predominant in the case of the O^-/NH_2^- formation, which shows the same behaviour as OH^-, with insignificant contribution at low collision energies, where the indoline anion dominates.
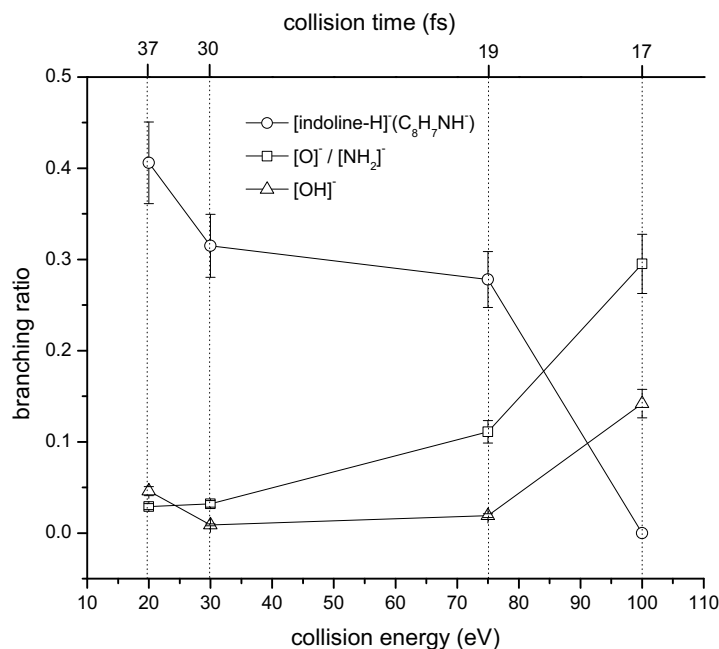
Figure 3. Branching ratios as a function of the lab frame collision energy for the dehydrogenated indoline anion ([indoline-H]$^-$), O$^-$/NH$_2^-$ and OH$^-$ fragments upon potassium-tryptophan collisions at 20, 30, 75 and 100 eV.

From Fig. 3 we see that the rearrangement process associated with formation of the dehydrogenated indoline anion benefits strongly from the longer transition times of the potassium at lower collision energies. The direct processes, on the other hand, are enhanced as the collision energy increases. In this context we note that at a lab-frame collision energy of 20 eV, the collision time amounts to 37 fs and E_{cm} is 10.8 eV. At a lab-frame collision energy of 100 eV, on the other hand, the collision time is shortened to 16 fs but E_{cm} amounts to 71.2 eV. Hence, while the direct processes predominantly depend on the energy transfer in the collision, the complicated rearrangement process leading to the formation of the dehydrogenated indoline anion is critically dependent on the lifetime of the collision complex. We attribute this observation to a stabilization of the transition state(s) through the interaction of the positively charged potassium ion and the intermediate anionic tryptophan formed in the electron transfer process. Such stabilization may partly be due to a general coulomb stabilization of the anion in the complex, but also to a preferable

geometry in the collision complex allowing for the required hydrogen transfer processes to proceed within its lifetime. We note that the dissociation channels observed are competitive channels and while the faster more direct processes benefit directly from increased energy transfer, rearrangement reactions such as the formation of the dehydrogenated indoline anion are critically dependent on reaching a favourable geometry for the respective rearrangement to proceed.

For further comparison, Fig. 4 shows the branching ratios for HO_2^-/NH_2OH^- and $CN^-/C_2H_2^-$ as a function of the collision energy. These ions do, at least in part, require some rearrangement and while the branching ratio for HO_2^-/NH_2OH^- has a maximum in the range from 30 to about 70 eV, the $CN^-/C_2H_2^-$ branching ratio decreases slightly with increasing collision energy, displaying a similar trend as is observed for the dehydrogenated indoline anion. Though the trends are not as clear here as for the fragments shown in Fig. 3, they still exhibit the interplay between the lifetime of the collision complex and the energy available for the dissociation to proceed.
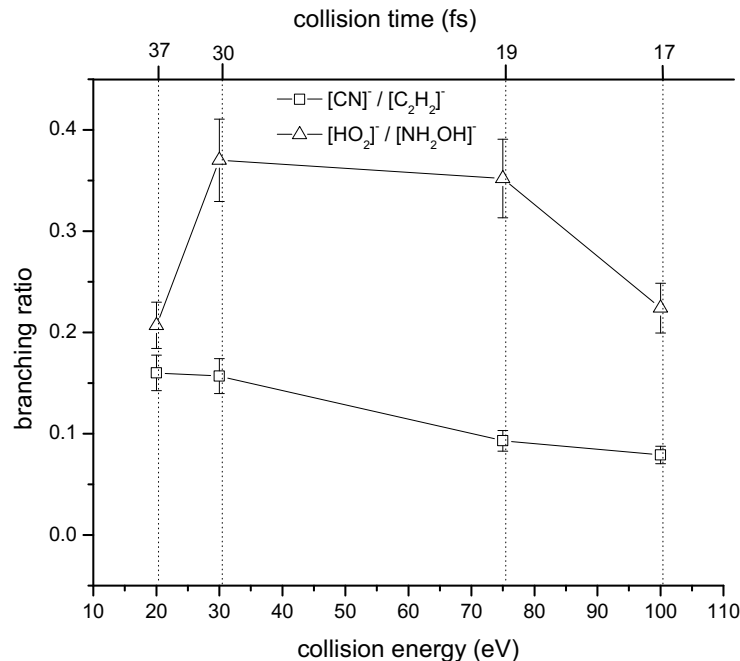
Figure 4. Collision energy dependence of the branching ratios for $CN^-/C_2H_2^-$ and HO_2^-/NH_2OH^- fragment formation upon potassium-tryptophan collisions at 20, 30, 75 and 100 eV in the laboratory-frame.

In order to further our knowledge on the underlying molecular mechanism responsible for the dehydrogenated indoline anion formation (m/z 118), comprehensive quantum chemical calculations were performed for a number of potential reaction pathways for this process.

In a potassium-tryptophan collision yielding the dehydrogenated indoline anion, cleavage of the C_β bond (see Fig. 2) from the side chain moiety and transfer of two hydrogens from the backbone to the indole moiety, must occur. To assess this reaction path we have initially explored, as a first step, a hydrogen transfer from the carboxylic group to different carbon acceptor positions in the indole ring, i.e. C_3, C_2 and C_{3a}. The resulting reaction paths are depicted in Fig. 5 (hydrogen transfer to C_3) and in Fig. S1 (hydrogen transfer to C_2) and Fig. S2 (hydrogen transfer to C_{3a}) in the Electronic Supplementary Information (ESI). The pathways shown in Fig. 5 and Fig. S1 show an initial hydrogen transfer from the carboxyl group to C_3 and C_2, respectively, leading to a C_3-C_β

bond cleavage, that in turn leads directly to the formation of m/z 117. For these two paths the gas-phase Gibbs free energy for the hydrogen transfer to C_2 shown in Fig. S1 is less favourable. In case of hydrogen transfer from the carboxyl group to C_3 shown in Fig. 5, the barrier for the hydrogen transfer is only 0.2 eV, and that for the C_3–C_β bond rupture is 0.6 eV with respect to the anion ground state (1.1 eV above the intermediate). The overall process leading to m/z 117 formation on this path is exergonic by 0.6 eV (see Fig. 5). For initial hydrogen transfer from the carboxyl group to C_2, shown in Fig. S1, we find the hydrogen transfer to be barrierless. The barrier for the C_3–C_β bond rupture, on the other hand, is found to be 2.5 eV and the reaction is endergonic by 1.7 eV (3.4 eV above the intermediate).

An initial hydrogen transfer from the carboxyl group to C_{3a} followed by a second hydrogen transfer from the NH_2 group to C_3, and a C_3–C_β bond rupture, shown in Fig. S2, leads to the formation of a m/z 118 fragment. The barrier for the initial hydrogen transfer on this path is only about 0.7 eV, but that for the second hydrogen transfer along with the C_3–C_β bond rupture is 4.3 eV (4.0 eV above the intermediate) and the overall reaction is endergonic by 1.3 eV.
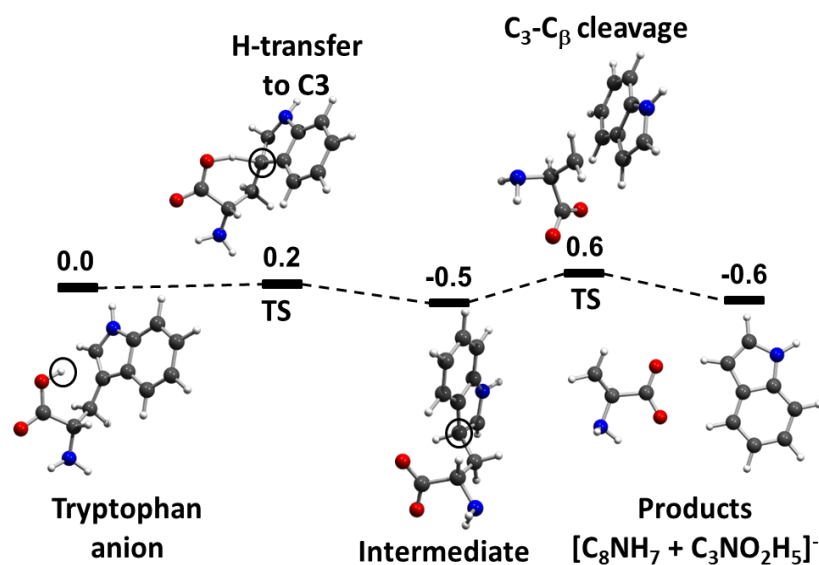
Figure 5. Gas-phase Gibbs free energy (eV), ΔG^0 298K, profile for the fragmentation mechanism of tryptophan upon electron transfer leading to a m/z 117 fragment. The initial hydrogen transfer is from the carboxylic group to C_3 at the indole moiety.

In the search for a more favourable path for the m/z 118 anion formation, we explored potential reaction pathways with an initial hydrogen transfer from C_α to C_{3a} (shown in Fig. 6) and hydrogen transfer from C_β to the C_2 carbon concomitant with a second hydrogen transfer from the carboxylic group to C_3 (shown in Fig. 7). For the initial hydrogen transfer from C_α to C_{3a}, shown in Fig. 6, the transition state (TS) is 2.5 eV above the anionic ground state and the intermediate formed is at 1.5 eV above the ground state. In a second step, the reaction may proceed from the intermediate state through excision of the C_3–C_β bond and concomitant hydrogen transfer from the carboxylic group to C_3 as shown in Fig. 6. The activation barrier for this step is 3.0 eV (1.5 eV above the intermediate). The overall reaction is endergonic by only 0.3 eV, but the resulting isomer of the

19

dehydrogenated indoline moiety on this path is hydrogenated at C_3 which annuls the aromaticity of the six-membered ring.
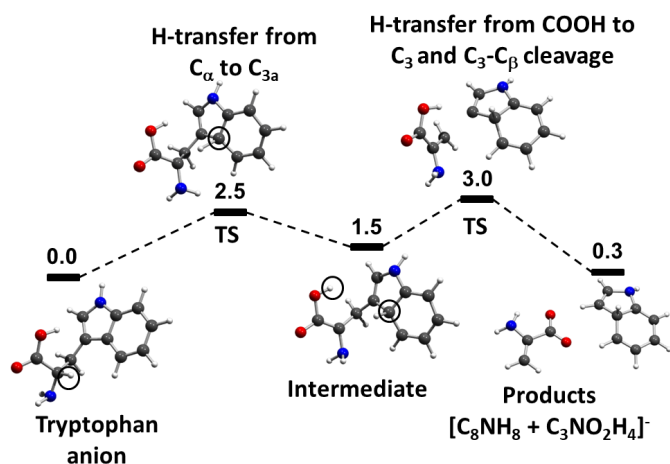

Figure 6. Gas-phase Gibbs free energy (eV), ΔG^0 298K, profile for the fragmentation mechanism of tryptophan upon electron transfer leading to fragment m/z 118. Hydrogen is transferred from the C_α to the C_{3a} carbon at the indole moiety. This is followed by hydrogen transfer from the carboxylic group to C_3 concomitant to C_3–C_β bond rupture.

For the reaction path initiated by hydrogen transfer from C_β to C_2 of the indole ring and hydrogen transfer from the carboxylic group to C_3 in the same step (shown in Fig. 7), we find the energy barrier for the first step to be 3.1 eV. However, the intermediate formed lies at 0.2 eV below the initial ground state. The second step leads to the formation of the de-hydrogenated indoline moiety through C_3-C_β bond breaking and the counter fragment forms a chiral (C_α) 3-member ring, with a positive formal charge on the N atom and a negative on the C_β atom. The barrier for this step is 2.7 eV and the overall reaction is endergonic by 1.7 eV.
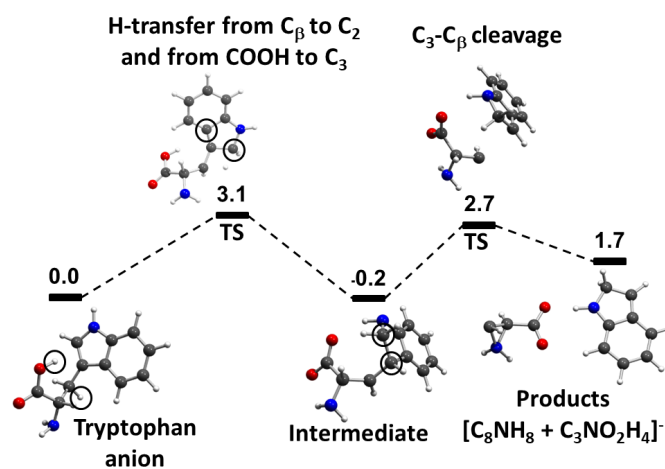
Figure 7. Gas-phase Gibbs free energy (eV), ΔG^0 298K, profile for the fragmentation mechanism of tryptophan upon electron transfer leading to m/z 118 formation. Two hydrogen atoms are transferred from the C_β to C_2 carbon and from the carboxylic group to C_3 of the indole moiety, followed by C_3-C_β bond cleavage.

For a laboratory frame collision energy of 20 eV, where m/z 118 formation is the most prominent feature (see Fig. 1), the available energy in the centre-of-mass frame is 10.8 eV, which is enough to allow both reaction pathways (Fig. 6 and Fig. 7) to be energetically accessible. This also applies to both reaction paths we calculated for the formation of the m/z fragment 117 shown in Figs. 5 and S1, as well as the energetically least favourable reaction path leading to the m/z 118 fragment (shown in Fig. S2). To further examine the progression along the reaction paths shown in Figs. 6 and 7 we have analysed the charge and spin density along these paths by means of Mulliken, Hirshfeld, APT, QM-5, Merz-Singh-Kollman and NBA/NBO approaches (see Tables S1 a and b and S2 a and b, for charge and spin density, respectively). Though there are variations between the different approaches, certain trends can be observed. It is clear that the additional charge is mainly located on the indole moiety of the initial tryptophan anion. However, in the transition state for the first hydrogen transfer, the charge is more delocalized while in the intermediate formed after hydrogen transfer, the charge is predominantly located on the carboxylic backbone. On the reaction path shown in Fig. 6, a certain delocalization is also found for the second transition state while for

the reaction path shown in Fig. 7, the charge remains on the backbone in this step. In both cases the charge retention is on the carboxylic fragment after the final bond rupture. This evolvement of the charge density along these reaction paths is also reflected in the resulting dipole moments (Mullikan) shown in table S3 a and b for the reaction path shown in Fig. 6 and Fig.7, respectively. On both these reaction paths, the spin density is on the indole site-chain moiety throughout the reaction, with the exception of the intermediate on the reaction path shown in Fig. 7, where the spin density is on the backbone.

Finally, to explore the influence of the potassium atom and that of the presence of a positive charge on the stability and charge distribution for the reaction products, additional calculations were carried out for the reaction products in the presence of a potassium atom and in the presence of a positive charge. Initially, energy minimisations of the products from the reaction path shown in Fig. 7 were carried out at the BHandHLYP/6-311++G(3df,2pd) level of theory, in the presence of the potassium atom. In these calculations, three locations of the potassium atom were explored; one, where the potassium atom was located 2.5 Å from the center of the 5-membered ring, one where the potassium atom was located 2.5 Å above the center of the 6-membered ring and one where the potassium atom was located 2.5 Å from the oxygen atoms of the carboxylic group. When the potassium atom was located 2.5 Å from the 5-membered ring it moves to the 6-membered ring in the optimization process, resulting in a similar geometrical configuration as when the potassium atom was initially located 2.5 Å above the plain of the 6-membered ring. The lowest energy configuration was found to be that of the optimized geometry with the potassium located in the proximity of the carboxylic group. The charge and spin density for the optimized products of the reaction paths shown in Fig. 6 and 7, with a potassium atom placed 2.5 Å from the carboxylic oxygens and for the same systems with a positive charge replacing the potassium atom were carried

out using the Mulliken, Hirshfeld, APT and QM-5 approach (see table 4S a and b and 5S). For both reaction paths with both the potassium atom and the positive charge, the charge density remained on the carboxylic backbone fragment.

From the current calculations it is clear that the energetics alone, when the influence of the potassium is not taken into account, do not explain the current observation of the dominant formation of the anionic m/z 118 fragment at low collision energies. Our observations, that the charge retention is on the side chain fragment is also in contrast to the charge density calculations, which predict the charge retention to be on the backbone fragment. Further, the stabilization of the end products in the presence of a potassium atom or a positive charge, does not, in our simplified approach, influence the charge distribution in the reaction products.

It is clear from the current comparisons that the influence of the potassium on the progression of the reactions cannot be explained by the extended lifetime of the TNI formed in the collision complex alone. Rather, the current study indicates that in the potassium tryptophan collisions certain transition states are stabilized in the collision complex which in turn alter the reaction pathways in such a way that they differ significantly from what is observed in free electron attachment. This is a dynamic problem and a better understanding may be obtainable via direct molecular dynamics simulations or via biased-sampling techniques. Such simulations would, however, be prohibitively expensive at the DFT level and exceed the scope for this study.

Conclusions

In this joint experimental and theoretical investigation, we have reported the collision energy dependence of the fragmentation of transient negative ions formed in collisions of neutral potassium atoms with neutral tryptophan molecules. The time-of-flight mass spectra give evidence

of the formation of the isobaric fragments $CN^-/C_2H_2^-$, O^-/NH_2^-, and HO_2^-/NH_2OH^- and the dehydrogenated indoline anion (m/z 118). From these, the branching ratios for the formation of O^-/NH_2^- and HO_2^-/NH_2OH^- increase significantly with increasing collision energy, lending support to a direct dissociation. The dehydrogenated indoline anion, on the other hand, is most significant at low collision energies and is absent at the highest collision energy probed (100 eV lab frame). This fragmentation path is not observed in free electron attachment experiments, and requires the transfer of two hydrogen atoms from the side chain to the indole group and cleavage of the C_β–C_3 bond of the side chain moiety. The most favourable reaction paths we identify for this process are an initial hydrogen transfer from C_β to C_2 of the indole ring followed by a hydrogen transfer from the carboxylic group to C_3 of the indole ring and an initial hydrogen transfer from C_α to C_3 of the indole ring, followed by hydrogen transfer from the carboxylic group to the indole ring. In both cases the charge retention after the cleavage of the C_3–C_β bond is found to be on the carboxylic backbone fragment. The energetically most favourable reaction path we computed is, however, an iInitial hydrogen transfer from the carboxylic group to the indole side chain, leading to direct cleavage of the C_3–C_β bond without the transfer of a second hydrogen, leading to the formation of a m/z 117 fragment. For this reaction path, the barrier for the hydrogen transfer from the carboxylic group to the C_3 position and the C_3–C_β bond rupture is only 0.6 eV, making this the lowest energy path of all paths considered.

It is thus clear that the calculations do not reflect the experimental observations and that the formation and evolution of the collision complex is determining for the transition states acquired in the process and thus the reaction path. This is a dynamic problem, which theoretical description requires molecular dynamics simulations or biased-sampling techniques. These approaches are computationally expensive but could initially be performed on more simple systems than the

current potassium tryptophan charge transfer process and could be benchmarked with the current results.

AUTHOR INFORMATION

Corresponding Author

* Corresponding authors: f.ferreiradasilva@fct.unl.pt (F. Ferreira da Silva),

plimaovieira@fct.unl.pt (P. Limão-Vieira)

Author Contributions

Experimental data collection, analysis and interpretation: F. Ferreira da Silva, T. Cunha, A. Rebelo, O. Ingólfsson, P. Limão-Vieira; Quantum chemical calculations: A. Gil, M. J. Calhorda; Draft preparation: F. Ferreira da Silva, O. Ingólfsson, A. Gil; Review and editing: F. Ferreira da Silva, O. Ingólfsson, A. Gil, M. J. Calhorda, G. García, P. Limão-Vieira

SUPPORTING INFORMATION

See the supporting information (SI) for details on the theoretical methods and computational procedures on the discussed tryptophan fragmentation pathways.

REFERENCES

(1)   Sjulstok, E.; Olsen, J. M. H.; Solov'yov, I. A. Quantifying Electron Transfer Reactions in Biological Systems: What Interactions Play the Major Role? *Sci. Rep.* **2015**, *5*, 18446.

(2)   Reece, S. Y.; Hodgkiss, J. M.; Stubbe, J.; Nocera, D. G. Proton-Coupled Electron Transfer: The Mechanistic Underpinning for Radical Transport and Catalysis in Biology. *Philos. Trans. R. Soc. London B Biol. Sci.* **2006**, *361* (1472), 1351–1364.

(3)   Gray, H. B.; Winkler, J. R. Electron Tunneling through Proteins. *Q. Rev. Biophys.* **2003**, *36* (3), 341–372.

(4)   Dempsey, J. L.; Winkler, J. R.; Gray, H. B. Proton-Coupled Electron Flow in Protein Redox Machines. *Chem. Rev.* **2010**, *110* (12), 7024–7039.

(5)   Darnell, J., Lodish, H., Baltimore, D. *Molecular Cell Biology*, 5th editio.; W. H. Freeman and company: New York, 1990.

(6)   Aubert, C.; Mathis, P.; Eker, a P.; Brettel, K. Intraprotein Electron Transfer between Tyrosine and Tryptophan in DNA Photolyase from Anacystis Nidulans. *Proc. Natl. Acad. Sci. U. S. A.* **1999**, *96* (10), 5423–5427.

(7) Jovanovic, S. V; Harriman, A.; Simic, M. G. Electron-Transfer Reactions of Tryptophan and Tyrosine Derivatives. *J. Phys. Chem*. **1986**, *90* (9), 1935–1939.

(8) Pagba, C. V.; McCaslin, T. G.; Veglia, G.; Porcelli, F.; Yohannan, J.; Guo, Z.; McDaniel, M.; Barry, B. A. A Tyrosine–Tryptophan Dyad and Radical-Based Charge Transfer in a Ribonucleotide Reductase-Inspired Maquette. *Nat. Commun*. **2015**, *6*, 10010.

(9) Kaushik, N. K.; Kaushik, N.; Attri, P.; Kumar, N.; Kim, C. H.; Verma, A. K.; Choi, E. H. Biomedical Importance of Indoles. *Molecules* **2013**, *18* (6), 6620–6662.

(10) Boudaïffa, B.; Cloutier, P.; Hunting, D.; Huels, M. a; Sanche, L. Resonant Formation of DNA Strand Breaks by Low-Energy (3 to 20 EV) Electrons. *Science* **2000**, *287* (5458), 1658–1660.

(11) Alizadeh, E.; Orlando, T. M.; Sanche, L. Biomolecular Damage Induced by Ionizing Radiation: The Direct and Indirect Effects of Low-Energy Electrons on DNA. *Annu. Rev. Phys. Chem*. **2015**, *66* (1), 379–398.

(12) Baccarelli, I.; Bald, I.; Gianturco, F. A.; Illenberger, E.; Kopyra, J. Electron-Induced Damage of DNA and Its Components: Experiments and Theoretical Models. *Phys. Rep*. **2011**, *508* (1–2), 1–44.

(13) Bald, I.; Denifl, S. The Role of Low-Energy Electrons in DNA Radiation Damage. In *Low-energy electrons Fundamentals and applications*; Ingólfsson, O., Ed.; Pan Stanford Publshing Pte. Ltd., 2019; pp 285–340.

(14) Sanche, L. Low Energy Electron-Driven Damage in Biomolecules. *Eur. Phys. J. D* **2005**, *35* (2), 367–390.

(15)   Ferreira Da Silva, F.; Denifl, S.; Märk, T. D.; Ellis, A. M.; Scheier, P. Electron Attachment to Amino Acid Clusters in Helium Nanodroplets: Glycine, Alanine, and Serine. *J. Chem. Phys.* **2010**, *132* (21), 214306.

(16)   Aflatooni, K.; Hitt, B.; Gallup, G. A.; Burrow, P. D. Temporary Anion States of Selected Amino Acids. *J. Chem. Phys.* **2001**, *115* (14), 6489–6494.

(17)   Borisevich, N. A.; Ivanov, A. L.; Kazakov, S. M.; Murtazaliev, D. V; Povedailo, V. A.; Khristoforov, O. V; Physics, A. INTERACTION OF ELECTRONS WITH INDOLE , TRYPTOPHAN , AND THEIR DERIVATIVES IN THE GAS PHASE. *J. Appl. Spectrosc.* **2005**, *72* (4), 503–508.

(18)   Abdoul-Carime, H.; Gohlke, S.; Illenberger, E. Fragmentation of Tryptophan by Low-Energy Electrons. *Chem. Phys. Lett.* **2005**, *402* (4–6), 497–502.

(19)   Vasil'ev, Y. V.; Figard, B. J.; Voinov, V. G.; Barofsky, D. F.; Deinzer, M. L. Resonant Electron Capture by Some Amino Acids and Their Methyl Esters. *J. Am. Chem. Soc.* **2006**, *128* (16), 5506–5515.

(20)   Scheer, A. M.; Mozejko, P.; Gallup, G. A.; Burrow, P. D. Total Dissociative Electron Attachment Cross Sections of Selected Amino Acids. *J. Chem. Phys.* **2007**, *126* (17), 174301.

(21)   Abdoul-Carime, H.; Sanche, L. Alteration of Protein Constituents Induced by Low-Energy (<40 EV) Electrons. III. The Aliphatic Amino Acids. *J. Phys. Chem. B* **2004**, *108* (1), 457–464.

(22)   Abdoul-carime, H.; Gohlke, S.; Illenberger, E. Degradation of N -Acetyl Tryptophan by

Low-Energy (<12 EV) Electrons. *J. Am. Chem. Soc. Am. Chem. Soc.* **2004**, *126*, 12158–12161.

(23)   Modelli, A.; Jones, D.; Pshenichnyuk, S. A. Electron Attachment to Indole and Related Molecules. *J. Chem. Phys.* **2013**, *139* (18).

(24)   Chiari, L.; Zecca, A.; Blanco, F.; García, G.; Brunger, M. J. Cross Sections for Positron and Electron Collisions with an Analog of the Purine Nucleobases: Indole. *Phys. Rev. A - At. Mol. Opt. Phys.* **2015**, *91* (1), 1–3.

(25)   Carles, S.; Desfrançois, C.; Schermann, J. P.; Smith, D. M. A.; Adamowicz, L. Structures and Electron Affinities of Indole–(Water)[Sub N] Clusters. *J. Chem. Phys.* **2000**, *112* (8), 3726.

(26)   Park, S. T.; Gahlmann, A.; He, Y.; Feenstra, J. S.; Zewail, A. H. Ultrafast Electron Diffraction Reveals Dark Structures of the Biological Chromophore Indole. *Angew. Chemie - Int. Ed.* **2008**, *47* (49), 9496–9499.

(27)   Denifl, S.; Flosadóttir, H. D.; Edtbauer, a.; Ingólfsson, O.; Märk, T. D.; Scheier, P. A Detailed Study on the Decomposition Pathways of the Amino Acid Valine upon Dissociative Electron Attachment. *Eur. Phys. J. D* **2010**, *60* (1), 37–44.

(28)   Mauracher, A.; Denifl, S.; Aleem, A.; Wendt, N.; Zappa, F.; Cicman, P.; Probst, M.; Märk, T. D.; Scheier, P.; Flosadóttir, H. D.; Ingólfsson, O.; Illenberger, E. Dissociative Electron Attachment to Gas Phase Glycine: Exploring the Decomposition Pathways by Mass Separation of Isobaric Fragment Anions. *Phys. Chem. Chem. Phys.* **2007**, *9* (42), 5680–5685.

(29)   Papp, P.; Urban, J.; Matejcík, S.; Stano, M.; Ingolfsson, O. Dissociative Electron Attachment to Gas Phase Valine: A Combined Experimental and Theoretical Study. *J. Chem. Phys.* **2006**, *125* (20), 204301.

(30)   Tseng, C. M.; Dyakov, Y. A.; Huang, H. C.; Huang, K. Y.; Lee, Y. T.; Ni, C. K.; Chiang, S. Y. Photodissociation Dynamics of Tryptophan and the Implication of Asymmetric Photolysis. *J. Chem. Phys.* **2010**, *133* (7), 1–4.

(31)   Antunes, R.; Almeida, D.; Martins, G.; Mason, N. J.; Garcia, G.; Maneira, M. J. P.; Nunes, Y.; Limão-Vieira, P. Negative Ion Formation in Potassium-Nitromethane Collisions. *Phys. Chem. Chem. Phys.* **2010**, *12* (39), 12513–12519.

(32)   Almeida, D.; Kinzel, D.; Ferreira da Silva, F.; Puschnigg, B.; Gschliesser, D.; Scheier, P.; Denifl, S.; Garcia, G.; Gonzalez, L.; Limao-Vieira, P. N-Site de-Methylation in Pyrimidine Bases as Studied by Low Energy Electrons and Ab Initio Calculations. *Phys. Chem. Chem. Phys.* **2013**, *15*, 11431.

(33)   Almeida, D.; Bacchus-Montabonel, M.-C.; Ferreira da Silva, F.; Garcia, G.; Limao-Vieira, P. Potassium-Uracil/Thymine Ring Cleavage Enhancement As Studied in Electron Transfer Experiments and Theoretical Calculations. *J. Phys. Chem. A* **2014**, *118* (33, SI), 6547–6552.

(34)   Ferreira da Silva, F.; Lança, M.; Almeida, D.; García, G.; Limão-Vieira, P. Anionic Fragmentation of Glycine upon Potassium-Molecule Collisions. *Eur. Phys. J. D* **2012**, *66* (3), 78.

(35)   Ferreira da Silva, F.; Rafael, J.; Cunha, T.; Almeida, D.; Limão-Vieira, P. Electron Transfer to Aliphatic Amino Acids in Neutral Potassium Collisions. *Int. J. Mass Spectrom.* **2014**,

365–366, 238–242.

(36)   Ferreira da Silva, F.; Meneses, G.; Ingólfsson, O.; Limão-Vieira, P. Side Chain Effects in Reactions of the Potassium-Tyrosine Charge Transfer Complex. *Chem. Phys. Lett.* **2016**, *662*, 19–24.

(37)   Ferreira da Silva, F.; Matias, C.; Almeida, D.; García, G.; Ingólfsson, O.; Flosadóttir, H. D.; Ómarsson, B.; Ptasinska, S.; Puschnigg, B.; Scheier, P.; Limão-Vieira, P.; Denifl, S. NCO-, a Key Fragment upon Dissociative Electron Attachment and Electron Transfer to Pyrimidine Bases: Site Selectivity for a Slow Decay Process. *J. Am. Soc. Mass Spectrom.* **2013**, *24* (11), 1787–1797.

(38)   Almeida, D.; Ferreira da Silva, F.; García, G.; Limão-Vieira, P. Selective Bond Cleavage in Potassium Collisions with Pyrimidine Bases of DNA. *Phys. Rev. Lett.* **2013**, *110* (January), 023201.

(39)   Prabhudesai, V. S.; Kelkar, A. H.; Nandi, D.; Krishnakumar, E. Functional Group Dependent Site Specific Fragmentation of Molecules by Low Energy Electrons. *Phys. Rev. Lett.* **2005**, *95* (14), 143202.

(40)   Ferreira da Silva, F.; Almeida, D.; Antunes, R.; Martins, G.; Nunes, Y.; Eden, S.; Garcia, G.; Limão-Vieira, P. Electron Transfer Processes in Potassium Collisions with 5-Fluorouracil and 5-Chlorouracil. *Phys. Chem. Chem. Phys.* **2011**, *13* (48), 21621–21629.

(41)   Frisch, M. J.; Trucks, G. W.; Schlegel, H. B.; Scuseria, G. E.; Robb, M. A.; Cheeseman, J. R.; Scalmani, G.; Barone, V.; Mennucci, B.; Petersson, G. A.; Nakatsuji, H.; Caricato, M.; Li, X.; Hratchian, H. P.; Izmaylov, A. F.; Bloino, J.; Zheng, G.; Sonnenberg, J. L.; Had, M.;

Fox, D. J. Gaussian 09. Gaussian, Inc.: Wallingford CT 2009.

(42)   Hanwell, M. D.; Curtis, D. E.; Lonie, D. C.; Vandermeersch, T.; Zurek, E.; Hutchison, G. R. Avogadro : An Advanced Semantic Chemical Editor , Visualization , and Analysis Platform. **2012**.

(43)   Halgren, T. A. MMFF VI. MMFF94s Option for Energy Minimization Studies. **2000**, *20* (7), 720–729.

(44)   Halgren, T. a. Force Fields for Conformational Interaction Energies and Geometries. *J. Comput. Chem.* **2000**, *20* (7), 730–748.

(45)   Gil, A.; Bertran, J.; Sodupe, M. Gas Phase Dissociation Energies of Saturated AHn·+ Radical Cations and AHn Neutrals (A = Li-F, Na-Cl): Dehydrogenation, Deprotonation, and Formation of AH·+n-2 - H2 Complexes. *J. Am. Chem. Soc.* **2003**, *125* (24), 7461–7469.

(46)   Gil, A.; Bertran, J.; Sodupe, M. Effects of Ionization on Bonds N-Glycylglycine Peptide: Influence of Intramolecular Hydrogen Bonds. *J. Chem. Phys.* **2006**, *124*, 154306.

(47)   Gil, A.; Simon, S.; Sodupe, M.; Bertran, J. Gas-Phase Proton-Transport Self-Catalysed Isomerisation of Glutamine Radical Cation: The Important Role of the Side-Chain. *Theor. Chem. Acc.* **2007**, *118* (3), 589–595.

(48)   Gil, A.; Simon, S.; Sodupe, M.; Bertrán, J. How the Site of Ionisation Influences Side-Chain Fragmentation in Histidine Radical Cation. *Chem Phys Lett* **2008**, *451*, 276–281.

(49)   Martínez-Núñez, E. An Automated Transition State Search Using Classical Trajectories Initialized at Multiple Minima. *Phys. Chem. Chem. Phys.* **2015**, *17* (22), 14912–14921.

(50)   Martínez-Núñez, E. An Automated Method to Find Transition States Using Chemical Dynamics Simulations. *J. Comput. Chem.* **2015**, *36* (4), 222–234.

(51)   MacQuarrie, D. A. *Statistical Mechanincs*; Rice, S. A., Ed.; Harper and Row: New York, 1986.

(52)   Galliot, A.; Gil, A.; Calhorda, M. J. Effects of Oxygenation on the Intercalation of 1,10-Phenanthroline-5,6/4,7-Dione between DNA Base Pairs: A Computational Study. *Phys Chem Chem Phys* **2017**, *19*, 16638–16649.

(53)   Gross, K. C.; Seybold, P. G.; Hadad, C. M. Comparison of Different Atomic Charge Schemes for Predicting PKa Variations in Substituted Anilines and Phenols. *Int. J. Quantum Chem.* **2002**, *90* (1), 445–458.

(54)   Mulliken, R. S. Electronic Population Analysis on LCAO - MO Molecular Wave Functions . III . Effects. **1970**, *2338* (1955).

(55)   Hirshfeld, F. L. Bonded-Atom Fragments for Describing Molecular Charge Densities. *Theor. Chim. Acta* **1977**, *44*, 129–138.

(56)   Cioslowski, J. AMERICAN CHEMICAL SOCIETY A New Population Analysis Based on Atomic Polar Tensors. *J. Am. Chem. Soc.* **1989**, *111* (22), 8333–8336.

(57)   Marenich, A. V; Jerome, S. V; Cramer, C. J.; Truhlar, D. G. Charge Model 5 : An Extension of Hirshfeld Population Analysis for the Accurate Description of Molecular Interactions in Gaseous and Condensed Phases. *J. Chem. Theory Comput.* **2012**, *8*, 527–541.

(58)   Besler, B. H.; Merz Jr., K. M.; Kollman, P. A. Atomic Charges Derived from Semiempirical

Methods. *J. Comput. Chem.* **1990**, *11* (4), 431–439.

(59)   Singh, U. C.; Kollman, P. A. An Approach to Computing Electrostatic Charges for Molecules. *J. Comput. Chem.* **1984**, *5* (2), 129–145.

(60)   Reed, A. E.; Weinstock, R. B.; Weinhold, F. Natural Population Analysis. *J. Chem. Physicsnal Chem. Phys.* **1985**, *83*, 735.

(61)   Muftakhov, M. V; Shchukin, P. V. Resonant Dissociative Electron Capture by the Simplest Amino Acids and Dipeptides. *Russ. Chem. Bull., Int. Ed.* **2010**, *59* (5), 896–911.

(62)   Vasil'ev, Y. V; Figard, B. J.; Barofsky, D. F.; Deinzer, M. L. Resonant Electron Capture by Some Amino Acids Esters. *J. Am. Chem. Soc.* **2007**, *268* (2–3), 106–121.

TOC